Int. J. New. Chem., 2023, Vol. 10, Issue 1, pp. 122-137.

International Journal of New Chemistry

Published online 2023 in http://www.ijnc.ir/.

Open Access

Print ISSN: 2645-7236

Online ISSN: 2383-188x

Original Research Article

Determination of optimum amounts of effective parameters in reactive dyes removal Using a zeolitic-imidazolate framework catalyst.

Shabnam Alibakhshi[1], Ashraf S. Shahvelayati[1*], Maryam Ranjbar[2*], Shabnam Sheshmani[1,] Saeid Souzangarzadeh[1]

[1]*Department of Chemistry, College of Basic Sciences, Yadegar-e- Imam Khomeini (RAH) Shahre Ray Branch, Islamic Azad University, Tehran, Iran*

[2]*Department of Chemical Technologies, Iranian Research Organization for Science and Technology (IROST), Tehran, Iran*

Received: 2022-06-20 *Accepted: 2022-8-23* *Published: 2022-9-16*

ABSTRACT

An efficient and rapid fabrication procedure for ZIF-8 crystals through ultrasonic assisted strategy (30min) was reported. Additionally, the crystallinity, morphology, chemical bonding, and porosity of ZIF-8 were fully characterized by XRD, and FT-IR. The Response surface methodology approach was established to optimize a series of adsorption conditions: initial concentration (10–400 mg/L), dose (0.02–1 g/L), and time (20–60 min) for Red 141 and Violet-5r removals. Particularly, plausible adsorption mechanisms (electrostatic interactions and π–π stacking) were elucidated, and isotherm models were rigorously studied by three-parameter equations (Langmuir, Freundlich, Tempkin). The adsorption isotherm data showed the adsorption of reactive dyes by ZIF-8, was consistent with the Langmuir isotherm model. The kinetics parameters were in accord with the pseudo-second-order equation, which implied that the adsorption rate was mainly controlled by the chemisorption mechanism. Through advantageous effectiveness involving good reusability (4 recycles), and maximum adsorption capacities (250-200 mg/g), it is recommendable to utilize ZIF-8 as a good adsorbent for the dyes remediation.

Keywords: Zeolitic-imidazolate frameworks, dyes remediation, response surface methodology, electrostatic interactions.

* Corresponding Author: Ashraf Shahvelayati email: avelayati@yahoo.com,
Maryam Ranjbar: email: marandjbar@irost.ir

1. Introduction

The untreated dye wastewater, due to its high toxicity and difficult biodegradability, has posed a significant, threat to the survival and safety of human beings and has become one of the significant obstacles to the sustainable development of human health, economy, and society [1-4]. Nowadays, tremendous demands on industrial and agricultural products have resulted in the intensive occurrence of potential pollutants (e.g., synthetic dyes) discharged into aqueous systems [5,6]. Wastewater containing these hazardous organic dyes can adversely influence the quality of water sources. Reactive azo dyes are widely used in textile industries and represent a large proportion of dyes discharged into the environment [7]. These azo dyes contain one or more azo (N=N) groups with heterocyclic and aromatic rings, and some functional groups, such as sulfonates and chloride. The azo groups within the structures of these dyes have low biodegradability and thus present many risks [8]. Therefore, removing these dyes before releasing them into the environment is necessary. Several methods, such as adsorption [9], photocatalysis [10], advanced oxidation processes [11], and coagulation [12], have been applied to remove these dyes before discharge into water. However, several disadvantages, such as consumption of energy and chemicals, complicated operation, high cost, and generation of toxic materials [13-15], limit the application of these techniques in wastewater treatment. Adsorption is considered one of the most efficient methods for removing contaminants because of its easy operation, non-generation of toxic materials, operational feasibility, low cost, and high efficiency [16, 17]. Generally; porous materials are superb sorbents that have a unique role in the removal of pollutions [18]. The adsorptive removal process is one of the initial suggested applications of these materials. Metal- organic frameworks (MOFs), also known as porous coordination polymers, are a relatively new class of highly porous materials, which possess a relative advantage compared to the other porous materials due to their unique properties, such as ultrahigh surface area, tunable and high porosity structures, the performance of pores and high crystallinity and designable organic ligands [19, 20]. Specifically, zeolitic imidazolate frameworks (ZIFs) are a subclass of metal-organic frameworks with zeolite or zeolite-like topologies, which have several remarkable features, such as chemical hardness and thermal stability [21]. Among different ZIFs materials, ZIF-8 has been employed for substantial works such as gas sorption [22], electrochemical biosensors [23], catalysis [24], and adsorptive removal of contaminants from liquids [25, 26]. Hence, ZIF-8 could be a good candidate as an attractive

adsorbent for dye removal due to its ultrahigh porosity, high chemical, and thermal stability, and hydrophobic nature. Surface modification of MOFs by loading appropriate functional groups or active spices, change in the interaction with functional groups [27]. Owing to the tunable porous network of ZIFs, several ZIFs, such as ZIF-67, ZIF-8, and ZIF-9, have been proven to be promising materials for dye adsorption [28-30].

In this study, the ZIF-8 crystals from Zn (NO3)2·6H2O and 2-HMim ligand were rapidly synthesized under ultrasonic irradiation conditions within 30 min. In particular, the molar ratio between Zn^{2+} and 2-HMim (1:1) was meager. The product was characterized using various techniques such as X-Ray diffraction (XRD), Fourier-transform infrared spectroscopy (FT–IR), etc. The response surface methodology approach could be adopted for optimizing the experimental parameters for the removal models of Red 141and violet-5r. The effect of concentration, solution pH, contact time, temperature, and dose of ZIF-8 on the adsorption capacity was vigorously clarified.

2. Material and Methods

All chemicals involving 2-methylimidazole (2-HMim), zinc (II) nitrate hexahydrate ($Zn(NO_3)_2.6H_2O$), and DMF were commercially purchased from Sigma-Aldrich and were used without further purification. Distilled water was used to synthesize and dilute the aqueous solutions. The dyes were purchased from Company Number: 3310350. The crystalline nature of ZIF-8 was analyzed by X-ray diffraction (model X'Pert PRO MPD, PANalytical, Made in the Netherland). Fourier transform-infrared (FT-IR) spectra were recorded (between 500 and 4000 cm^{-1}) on KBr pellets with a Tensor 27 Bruker spectrophotometer. To the concentration of the dye, a double beam UV-visible spectrophotometer was used (Cary 60, Agilent Technologies, and the USA). To estimate the pH of solutions, a pH meter was used (S47-K seven Multi, Mettler-Toledo, and Columbus, OH, USA).

2.1. Preparation of ZIF-8

In a typical preparation, a solid mixture of zinc nitrate hexahydrate ($Zn(NO_3)_2.6H_2O$) (3.74 g, 12.66 mmol) and 2-methylimidazole (H-MeIM) (1.2 g, 11.64 mmol) was dissolved in 45 mL of N, N′-dimethyl formamide (DMF), under ultrasonic condition. The autoclave was tightly capped and heated at a rate of 5 C/min to 140 °C in a programmable oven and held at this temperature for 24 h, then cooled at a rate of 40 °C/min to room temperature. After the removal of the mother

liquor from the mixture, chloroform (15 mL) was added to the vial. Colorless polyhedral crystals were collected from the upper chloroform layer, and washed with DMF (3 × 15 mL) for 2 days. The residual solvents were removed under vacuum at 200 °C for 6 h, yielding 1.2 g of white polyhedral crystals (80.62 % based on 2-methylimidazole).

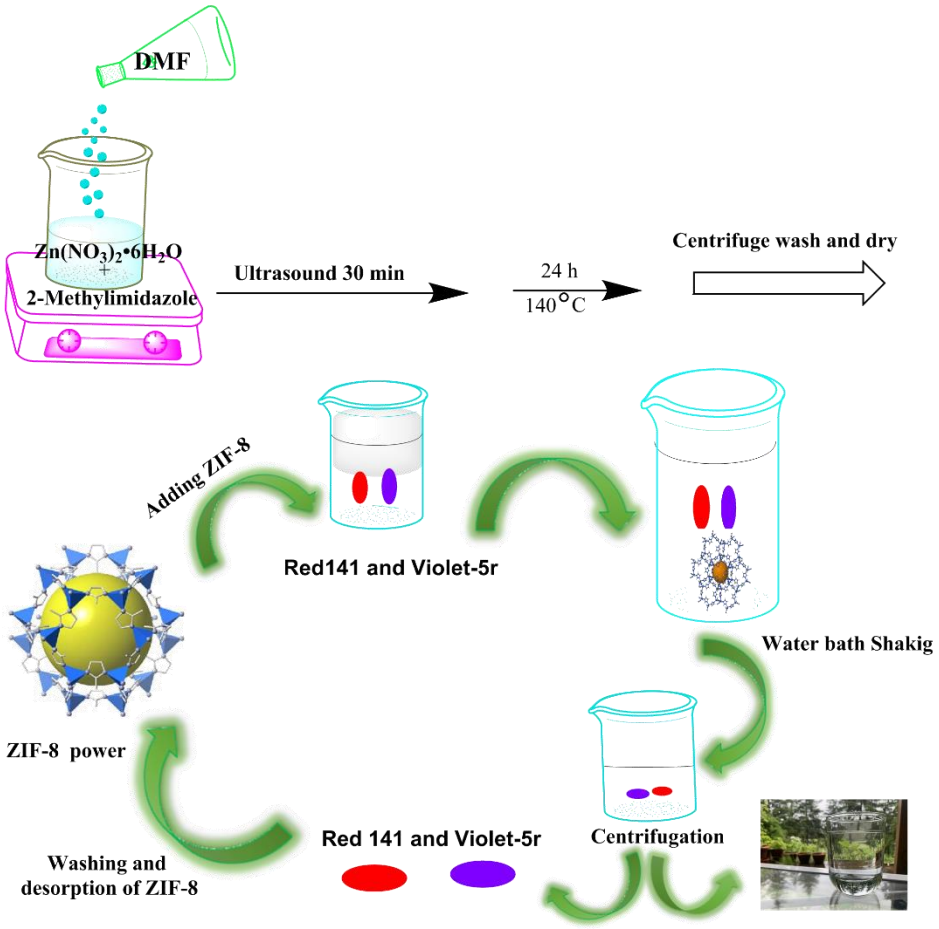

Figure 1. The preparation of ZIF-8

2.2. Adsorption study

An aqueous solution having variable concentrations of Red 141 and Violet-5r dye was used as simulated wastewater for examining the adsorption characteristics of ZIF-8 composites. Red 141 and Violet-5r were dissolved in deionized water and diluted to the required concentrations. The concentration of the Red 141 and Violet-5r solution after adsorption was analyzed using a UV–vis spectrophotometer (Cary 60, Agilent Technologies, and the USA). Subsequently, the

amounts of the adsorbed dye at a different times (qt, mg/g) and percent removal efficiency of Red 141 and Violet-5r paints were calculated according to the following equations.

$$\text{removal}\% = \frac{C_0 - C_e}{C_0} \quad (1)$$

$$q_t = \frac{(C_0 - C_t) \times V}{m} \quad (2)$$

C_0, C_e, and C_t (mg. L^{-1}) were the concentration of Red 141, and Violet-5r at initial, equilibrium, and at a different times (t, min), respectively. V was the volume of the Red 141, and Violet-5r solution, and m (g) was the mass of ZIF-8. To evaluate the adsorption capacity, and study kinetics properties, the dosage concentration of the adsorbent (0.02, 0.06, 0.08 and 1 mg. L^{-1}) and the concentration of the initial dye solution (10, 20, 30, 50, 100, 150, 200, 250, 300, 350 and 400 mg. L^{-1}) were selected.

3. Result and discussion

3.1. Characterization of ZIF-8

Textual features of the material were characterized using physicochemical analytic techniques comprising XRD diffraction, and FT-IR spectrum. Firstly, our findings were confirmed by the crystalline structure of the ZIF-8 sample ,as X-ray diffraction shown in Fig. 2. Major summits at 2θ = 9.94° (011), 10.37° (002), 12.72° (112), 14.73° (022), 16.50° (013), 18.21° (022), 26.71° (134), 31.79° (235), and 36.27° (400) are observed, which could be in excellent agreement with the theoretically calculated pattern from a recent study [31].

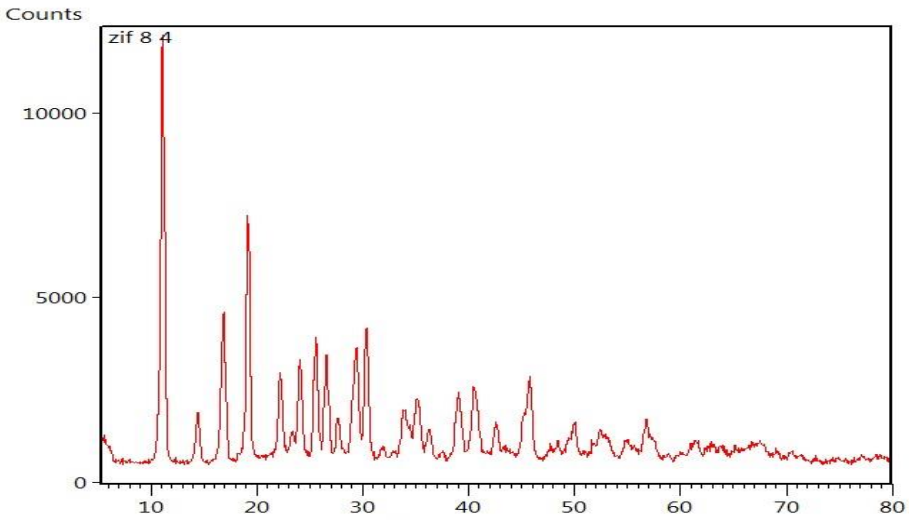

Figure 2. XRD images of ZIF-8 [31]

Fig. 3 provides more evidence, of chemical bonds inherent in the ZIF-8 structure. The most fundamental footprint stretched at around 430.5 cm^{-1} may be attributed to Zn–N coordination bonding [32]. The characteristic peaks at 742 and 1425 cm^{-1} were related to the H-aromatic part; a single at 2929 cm^{-1} could be ascribed by aliphatic C–H vibration. Another sharp footprint at 1586.73 cm^{-1} is highly likely unsaturated C=C chemical bonds.

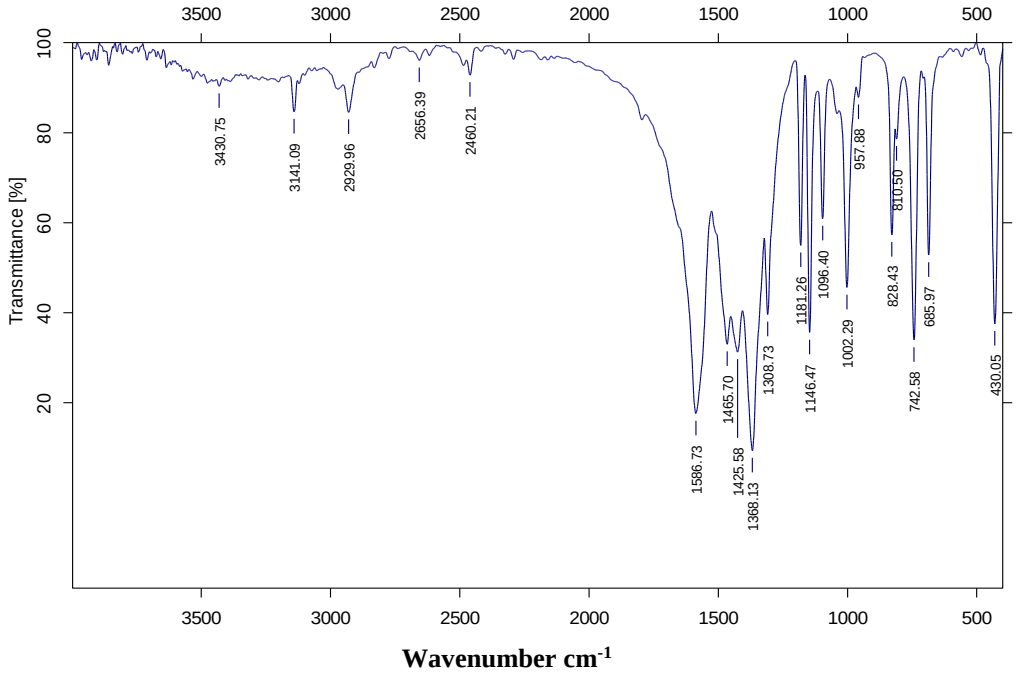

Figure 3. FTIR images of ZIF-8

3.2. Adsorption of reactive dyes by ZIF-8

3.2.1 Effect of several factors on adsorption capacity by ZIF-8

Adsorption capacity is an important indicator to assess how much an adsorbent can capture Red 141 and Violet-5r dyes molecules through the adsorption occurring heterogeneous phase (liquid/solid); herein, the most influential factors involving contact time (20–60 min), ZIF-8 dose (0.02–1.0 g/L), solution pH (2–10), and initial concentration (10–400 mg/L) were investigated. Graphical data for these four factors were illustrated in Fig. 4. According to Fig. 4(a), the adsorption capacities soared at the first 60-min moment. The equilibrium states were shown as 60 min for Red 141 and Violet-5r dyes. These findings perfectly correspondent with optimization results obtained from response surface methodology. The effect of the ZIF-8 dose on the uptake of Red 141 and Violet-5r was shown in Fig. 4(b). A considerable deduction was

observed when increasing the amount of ZIF-8 adsorbent (0.02–1 g/L). Therefore, the present study fixed the optimum dose of ZIF-8, at 1 g/L for the adsorption of both dyes. It was found that the adsorption of Red 141 was better than that of Violet-5r at higher concentrations (Fig. 4(c)).

As shown in Fig. 4(d), the adsorption capacity of ZIF-8 increased with the increasing temperature. According to Fig. 4(e), the maximum adsorption capacity occurred at pH 2 due to the neutralization of the OH^- groups by the hydrogen ions and favors the adsorption of reactive Red 141 and Violet-5r. At higher pH, the presence of more significant OH^- hinders the retention of Red 141 and Violet-5r because of the increase in negatively charged sites which creates an electrostatic repulsion and a competition between the OH^- and the active areas of the dyes (R^-SO3).

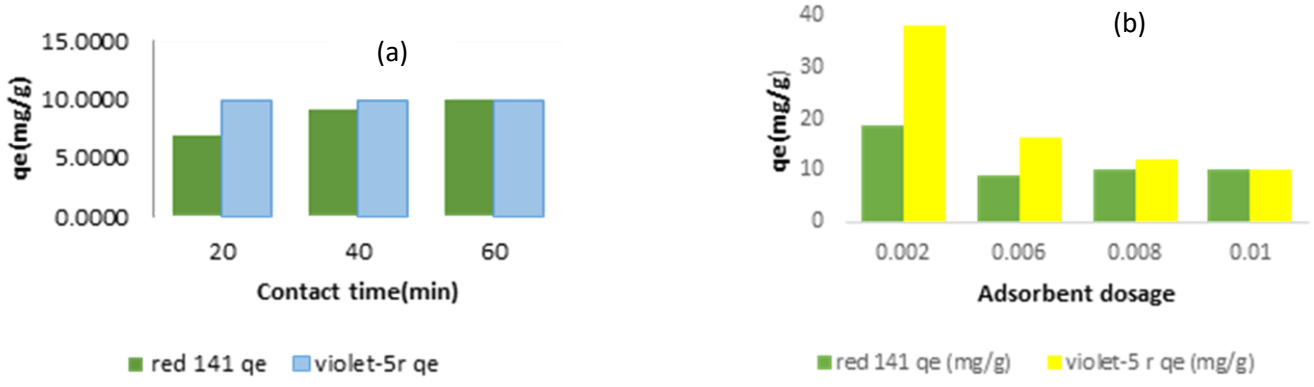

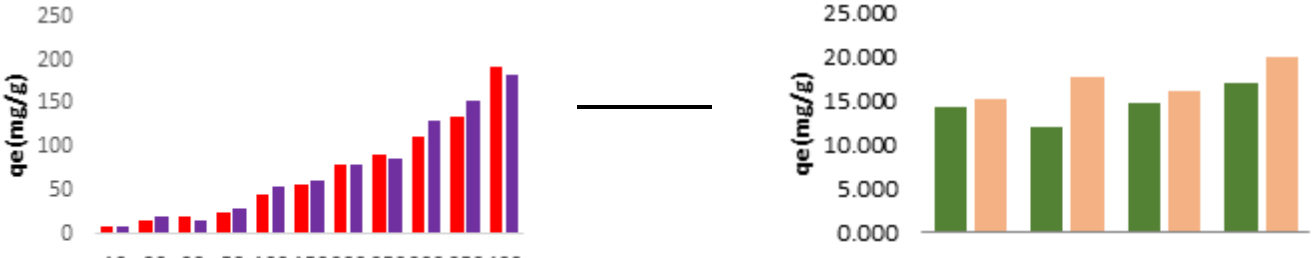

(c) (d)

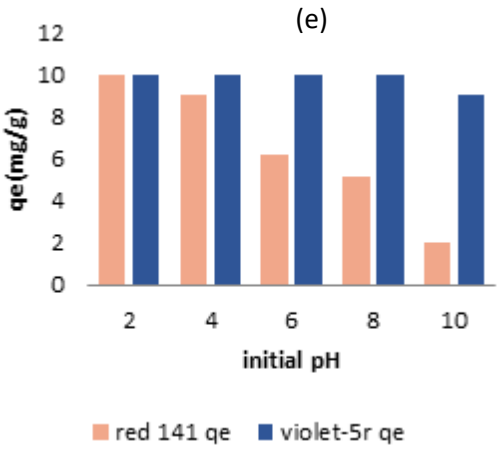

Figure 4. Effect of contact time (a), ZIF-8 dose (b), initial concentration (c) temperature (d), and solution pH (e) on Red 141 and Violet-5r adsorption capacities.

3.3 Adsorption isotherm

Equilibrium Data are the basis of the adsorption systems designed to remove organic contaminants commonly known as adsorption isotherms. In general, adsorption isotherms such as Langmuir, Freundlich, and Tempkin provide valuable information about adsorption mechanism, surface properties and the tendency of the adsorbents [33].

The Langmuir adsorption isotherm describes the equilibrium between the surface of the adsorbent and solution in the form of reversible chemical balance. This model assumes that the adsorption process occurs in the specific and homogeneous sites on the absorbent surface without any transmission of adsorbate in the plane of the character. The linear form of the Langmuir isotherm is shown in the following equation [34].

$$\frac{1}{q_e} = \frac{1}{Q_{max}} + \frac{1}{bQ_{max}}\left(\frac{1}{C_e}\right) \quad (3)$$

Where qe (mg. g^{-1}) and Ce (mg. L^{-1}) are the amount of dye adsorbed per unit mass of ZIF-8 and the dye concentration in solution at equilibrium, respectively. qm (mg. g^{-1}) is the maximum adsorption capacity, and K_L (b) ($L.mg^{-1}$) is Langmuir constant related. Dependence of adsorbent and adsorbate. The adsorption isotherm constants (Q_0, K_L, and R^2) were obtained from the linear plotting of $1/C_e$ versus $1/q_e$ data for the Langmuir model using ZIF-8 (Table1). According to correlation coefficient R^2 values, the Longmuir isotherm fitted the experimental data better than all other models. Freundlich isotherm is based on monolayer, non-ideal and reversible adsorption, which can be used for multiple-layer adsorption on the heterogeneous, surfaces with disparate adsorption energy and affinities. This model can be expressed by:

$$q_e = K_f C_e^{\frac{1}{n}} \quad (4)$$

K_F and 1/n are Freundlich constants related to adsorption capacity per unit concentration and adsorption intensity, respectively. The value of n indicates the favorability of adsorption. If n>1, the nature of adsorption is favorable. The rearranged form of Eq. (5) in linear form is:

$$\log q_e = \log K_f + \frac{1}{n}\log C_e \quad (5)$$

The Freundlich isotherm of reactive dye removal from a single system was studied by linear plotting log q_e against log Ce at different adsorbent dosages. Table 1 presents the isotherm constants (K_F, n, and R^2). The values of n for all cases were more significant, than 1, representing the calm nature of adsorption.

The Tempkin isotherm model presumes that the adsorption heat decreased linearly with increasing the coverage of the absorbent surface. The uniform distribution of the binding energy is one of the features of this model. The linear form of this isotherm is described as:

$$q_e = \frac{RT}{b_T}\ln k_T + \frac{RT}{b_T}\ln C_e \quad (6)$$

Where b_T is the Tempkin constant indicated sorption power (kJ mol^{-1}), and K_T is the equilibrium binding constant related to the maximum binding energy (L g^{-1}), R is the gas constant (8.314 J mol^{-1} K^{-1}). T is the absolute temperature (K). The compatibility of Tempkin isotherm with dye adsorption data using ZIF-8 was studied by linear plotting q_e versus ln C_e. The isotherm constants (A_T, B_T, and R^2) are listed in Table 1. These values are lower than the Freundlich and Langmuir

values which indicate that the Tempkin isotherm has a worse fit of experimental data than other isotherms.

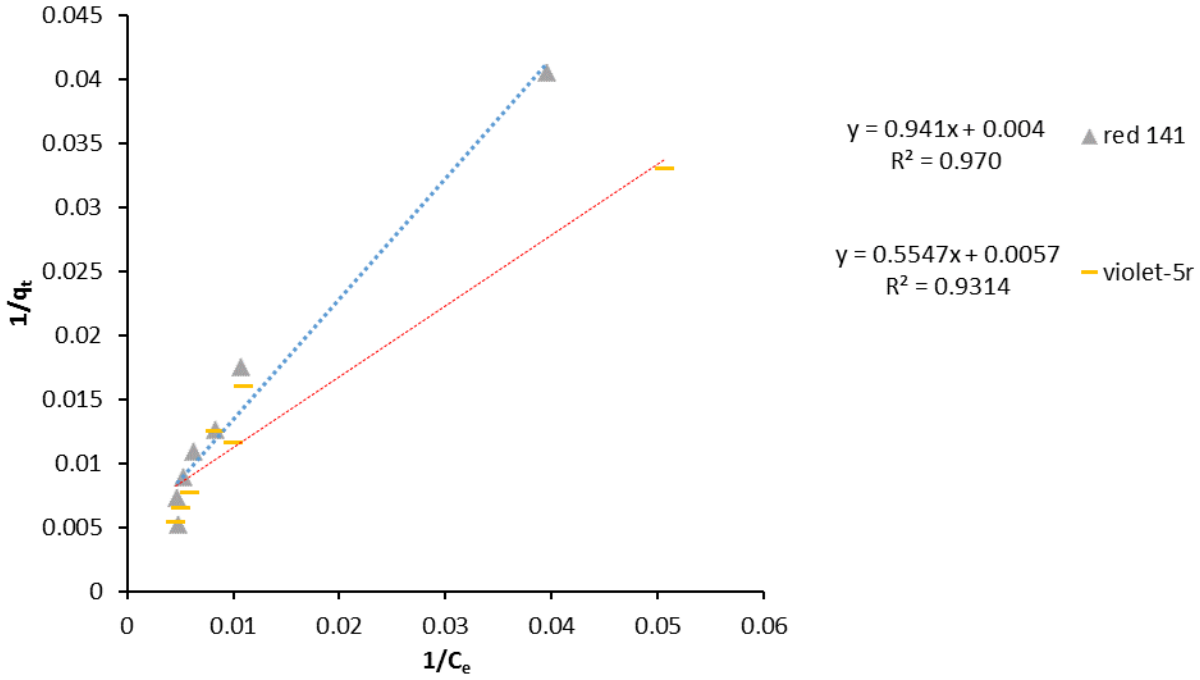

Figure 5. Linearized Langmuir isotherm for the adsorption of reactive dyes by ZIF-8 composites.

Table 1. Linearized isotherm coefficients for dye adsorption at different adsorbents (0.01g) Dosage and 50-400 mg/L dye concentrations (10 mL solution, pH=2, temperature = 65°C, contact time time=60min).

Isoterm Models	Isoterm parameters	Red 141	Violet-5r
Langmuir model	Q_m(mg/g) K_L (L/mg) R^2	250 0.004250 0.970	200 0.009025 0.931
Freundlich model	K_f (L/mg) n R^2	1.445 1.182 0.922	3.311 1.432 0.868
Tempkin model	K_T(L/mg) b_T(J/mol) R^2 B_1	0.0436 47.34 0.672 59.36	0.0621 52.77 0.652 53.25
Separation factor (R_L)	C_0 (mg/L) 50 400	 0.82 0.37	 0.68 0.21

Table 2. Comparison of the adsorption capacity of reactive dyes by various adsorbents.

Adsorbents samples	q_{max} (mg/g)	Ref
Red 141		
Pyrrhotite Ash	5.07	[35]
Nickel oxide doped	38.91	[36]
Comcob activated carbon	2.86	[37]
New ZIF-8	250	This study
Violet_5r		
Activated coal obtains from orange peel	185.1	[38]
Bent-NH_2/TOL	30.9	[39]
Bent-NH_2/HEX	60.9	[39]
New ZIF-8	200	This study

3.4 Adsorption kinetics study

Pseudo-first-order reaction model. The integrated form of the pseudo-first-order kinetic model based on the solid capacity for sorption analysis is of the form:

$$\ln(q_e - q_t) = \ln q_e - k s_1 t \quad (7)$$

Therefore, Eq. (7) infers a linear plot of ln (q_1-q_t) vs. time (t). The linear fit correlation coefficient of the determinant. This is the integrated rate law for a pseudo-second-order reaction. Rearranging Eq. (9) obtains

$$\frac{1}{(q_e - q_t)} = \frac{1}{q_e} + kt \quad (8)$$

$$\frac{t}{q_t} = \frac{1}{h} + \frac{1}{q_e} t \quad (9)$$

Where h = k q_e^2Eq. (5) Indicates that a linear plot of t/q_t vs. time (t) confirms that the reaction rate followed pseudo-second-order kinetics (Fig. 6). Based on the coefficient of the determinant of values, the adsorption processes followed the pseudo-second-order reaction kinetic model better than the other three kinetic models.

Adsorption is a multi-stage process involving the transfer of solute molecules from the aqueous phase to the surface of solid particles and subsequently penetrating the pores (slow step and speed determinative), respectively. First and second-order kinetic models cannot determine the

diffusion mechanism, so it is preferred to evaluate the results of kinetic with an intraparticle diffusion model. This kinetic model can be expressed using the following equation: [40]

$$q_t = k_p t^{1/2} + I \quad (10)$$

Where kp (mg g^{-1} $min^{-0.5}$) is the intraparticle diffusion rate constant, and I am the intercept .Table 3 shows the intraparticle diffusion kinetics constants (k_p, I, and R^2) obtained by linear plotting q_t against $t0^{.5}$. The Elovich equation is another kinetic model equation based on the adsorption capacity expressed as follows: [41]

$$q_t = \frac{1}{\beta}\ln(\alpha\beta) + \ln(t) \quad (11)$$

Where α and β are the Elovich constants and represent the initial adsorption rate (g $mg^{-1}min^{-1}$) and the desorption constant (mg g^{-1} min^{-1}), respectively. The Elovich constants could be obtained from the graphs of q_t versus ln t (Table 3).

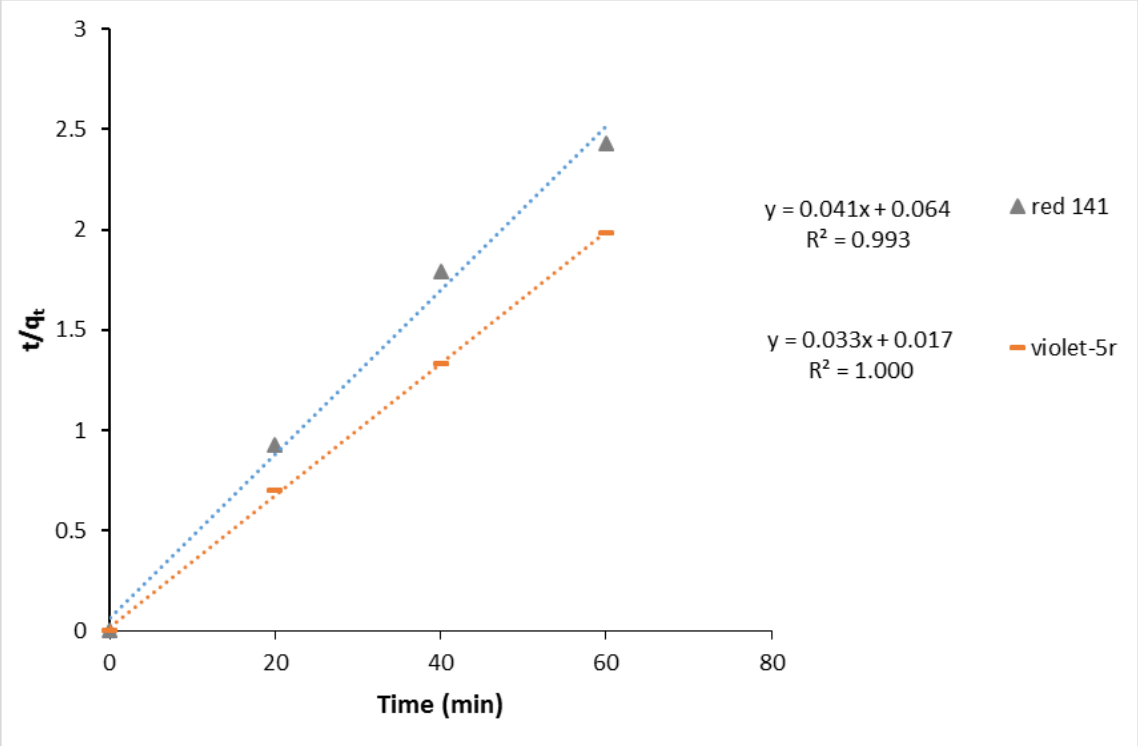

Figure 6. Kinetics plot for the adsorption of reactive dyes bye ZIF-8. The pseudo- order-model (contact time=20-60 min, temperature= 65°C, adsorbent mass=0.01g, 50mg/L, Stirring=400 rpm, and pH=2).

Table3. Kinetics constants for the adsorption of reactive dyes by ZIF-8(C) (contact time=20-60 min, temperature= 65°C, stirring=400 rpm and pH=2).

		Red 141	Violet-5r
Pseudo – first – order model	$q_{e,exp}$(mg/g)	24.68	30.27
	$q_{e,cal}$(mg/g)	18.39	25.79
	K_1(min^{-1})	0.059	0.0118
	R^2	0.843	0.986
Pseudo – second – order model	$q_{e,cal}$(mg/g)	24.39	30.30
	K_2(g/min.mg)	0.026	0.064
	R^2	0.993	1
Intra-particle diffusion model	K_p(g/min.mg)	0.938	0.555
	C(mg/g)	17.055	26.165
	R^2	0.883	0.909
Elovich constants	R^2	0.834	0.945
	α (Mg/g.min)	364.80	2340724.13
	ß (g/mg)	0.371	0.599

3.5 Recycle and regeneration of ZIF-8 nanocomposites

The practical potential for adsorbents can be substantially assessed through their recyclability studies. Herein, these experiments were carried out by recycling ZIF-8 under the optimized conditions: ZIF-8 dose of 1 g/L, 10 mL Violet-5r solution at 10 mg/L and pH = 2, contact time of 60 min, and under agitation (200 rpm). The procedure was described in the following step. The ZIF-8 adsorbent utilized for the first experiment was separated by the centrifugation technique. Then the solid was immersed in ethanol (3×20 mL) and rewashed with distilled water (3×20 mL) to remove Violet-5r dye molecules from the ZIF-8 structure. After drying the adsorbent ,the experiment was repeated, resembling the above standards. Initial and final Violet-5r concentrations were determined by UV–Vis spectrophotometer at 560 nm. The outcomes in Fig. 7 indicate that ZIF-8 can be reused at least 4 times with very moderate change after each recyclability run.

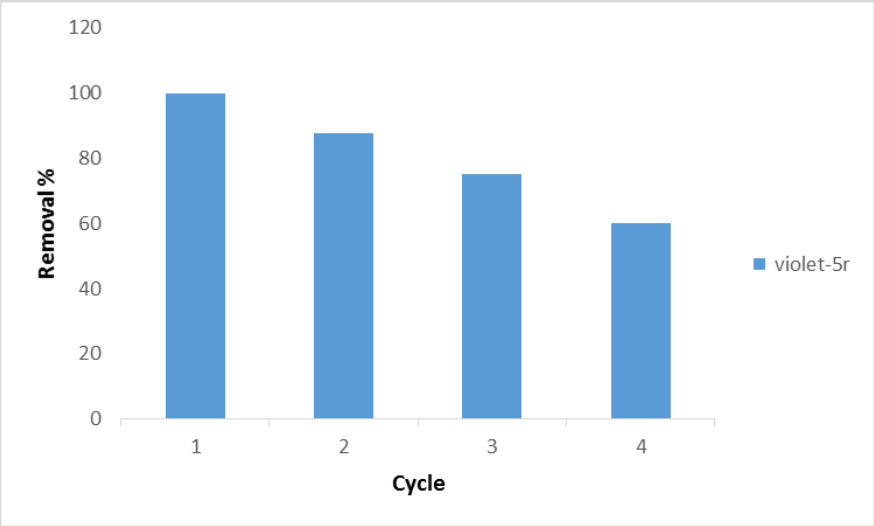

Figure 7. Recycled adsorption of RD_2, RD_6 and RD_7 (20 mg/L, by ZIF-8(C) 0.01 g)

4. Conclusions

The ZIF-8 was successfully synthesized by the solvothermal method. According to the results of response surface methodology-based optimization, the optimal conditions to eliminate Red 141, and Violet-5r were Co = 10 mg/L, contact time=60 min, adsorbent dosage=1 g/L, and pH=2, T=65°. For the dyes above, ZIF-8 showed superior adsorption capacity at 250 and 200 mg/g in comparison with other adsorbents. The adsorption kinetics followed the pseudo-second-order models for two these dyes. According to the adsorption isotherms, the colors follow the Langmuir model. The exceptional adsorption properties of ZIF-8 can be attributed largely to the unique structure and interaction of active functional groups, such as electrostatic interaction, hydrogen bonding, π–π conjugation, and coordination effect of zinc. Based on the thermodynamic parameters, the adsorption on ZIF-8 was spontaneous and favorable from a thermodynamic perspective. Red 141 and Violet-5r dyes were removed by this adsorptant in an exothermic manner. The adsorption process was greatly influenced by temperature, which affected the viscosity of the solution and, therefore, the adsorption capacity. With its unique properties, such as high recycling capacity, aromatic rings, and high removal efficiency, ZIF-8 is a highly efficient dye adsorbent for waste water dye removal.

5. **Acknowledgements**

The author would like to thank the Islamic Azad University of Yadegar-e-Imam Khomeini (RAH) Shahre-Rey branch for giving a grant to carry out the project mentioned above.

Reference

[1] J. An, H. Chen, S. Wei, J. Gu, Environ. Earth Sci., 74, 5077 (2015).
[2] A.K. Mishra, Sol-Gel Based Nanoceramic Materials: Preparation, Properties and Applications, (2016).
[3] A.G. Tafti, A. Rashidi, M.E. Yazdanshenas.,8, 515 (2021).
[4] M. Mozafarjalali, M. Hajiani, A. Haji, Int. J. New Chem., 7, 111 (2020).
[5] N. Tara, S.I. Siddiqui, G. Rathi, S.A. Chaudhry, Inamuddin, A.M. Asiri, Curr. Anal. Chem., 16, 14 (2019).
[6] M.P. Foroush, R. Ahmadi, M. Yousefi, J. Najafpour, South African J. Chem. Eng., 37, 135 (2021).
[7] A. Sharma, Z. Syed, U. Brighu, A.B. Gupta, C. Ram, J. Clean. Prod., 220, 23 (2019).
[8] W. Konicki, M. Aleksandrzak, D. Moszyński, E. Mijowska, J. Colloid Interface Sci., 496, 188 (2017).
[9] R.A. Rashid, M.A. Mohd, Kasim Mohammed Hello, Sci. Lett., 12, 301 (2018).
[10] A.H. Jawad, N.S.A. Mubarak, M.A.M. Ishak, K. Ismail, W.I. Nawawi, J. Taibah Univ. Sci., 10, 352 (2016).
[11] P. V. Nidheesh, M. Zhou, M.A. Oturan, Chemosphere., 197, 210 (2018).
[12] N. de C.L. Beluci, G.A.P. Mateus, C.S. Miyashiro, N.C. Homem, R.G. Gomes, M.R. Fagundes-Klen, R. Bergamasco, A.M.S. Vieira, Sci. Total Environ., 664, 222 (2019).
[13] M. Ahmadi, M. Hazrati Niari, B. Kakavandi, J. Mol. Liq., 248, 184 (2017).
[14] M. Ahmadi, M. Foladivanda, N. Jaafarzadeh, Z. Ramezani, B. Ramavandi, S. Jorfi, B. Kakavandi, J. Water Supply Res. Technol. - AQUA., 66, 116 (2017).
[15] B. Kakavandi, A. Takdastan, S. Pourfadakari, M. Ahmadmoazzam, S. Jorfi, J. Taiwan Inst. Chem. Eng., 96, 329 (2019).
[16] M. Kermani, H. Izanloo, R.R. Kalantary, H.S. Barzaki, B. Kakavandi, Desalin. Water Treat., 80, 357 (2017).
[17] N.H. Abdullah, K. Shameli, E.C. Abdullah, L.C. Abdullah, Compos. Part B Eng., 162, 538 (2019).
[18] I. Ahmed, S.H. Jhung, Mater., Today 17, 136 (2014).
[19] O.M. Zhou, H. C., Long, J. R., & Yaghi, Chem. Rev., 112, 673 (2012).
[20] J.R. Li, J. Sculley, H.C. Zhou, Chem. Rev.,112, 869 (2012).
[21] S.K. Nune, P.K. Thallapally, A. Dohnalkova, C. Wang, J. Liu, G.J. Exarhos, Chem. Commun., 46, 4878 (2010).
[22] H. Bux, F. Liang, Y. Li, J. Cravillon, M. Wiebcke, J. Caro, J. Am. Chem. Soc., 131, 16000 (2009).
[23] G. Lu, J.T. Hupp, J. Am. Chem. Soc., 132, 7832 (2010).
[24] A.N. Ökte, D. Karamanis, E. Chalkia, D. Tuncel, Mater. Chem. Phys., 187, 5 (2017).
[25] J.Q. Jiang, C.X. Yang, X.P. Yan, ACS Appl. Mater., Interfaces 5, 9837 (2013).
[26] K.Y.A. Lin, Y.C. Chen, S. Phattarapattamawong, J. Colloid Interface Sci., 478, 97 (2016).
[27] S. Wuttke, S. Braig, T. Preiß, A. Zimpel, J. Sicklinger, C. Bellomo, J.O. Rädler, A.M. Vollmar, T. Bein, Chem. Commun., 51, 15752 (2015).

[28] T.-T. Han, H.-L. Bai, Y.-Y. Liu, J.-F. Ma, New J. Chem.,42, 717 (2018).
[29] Y. Li, K. Zhou, M. He, J. Yao, Microporous Mesoporous Mater., 234, 287 (2016).
[30] R. Qiang, Y. Du, D. Chen, W. Ma, Y. Wang, P. Xu, J. Ma, H. Zhao, X. Han, J. Alloys Compd., 681, 384 (2016).
[31] S. Tanaka, K. Fujita, Y. Miyake, M. Miyamoto, Y. Hasegawa, T. Makino, S. Van Der Perre, J. Cousin Saint Remi, T. Van Assche, G. V. Baron, J.F.M. Denayer, J. Phys. Chem., C 119, 28430 (2015).
[32] M. Adnan, K. Li, L. Xu, Y. Yan., Catalysts 8 (2018).
[33] E.R. Alley., Environment 1., 32, 191 (2007).
[34] N.M. Mahmoodi, J. Abdi, F. Najafi, J. Colloid Interface Sci., 400, 88 (2013).
[35] K.-Y. Andrew Lin, W.-D. Lee, Chem. Eng. J., 284, 1017 (2016).
[36] G.E. do Nascimento, M.M.M.B. Duarte, N.F. Campos, O.R.S. da Rocha, V.L. da Silva, Environ. Technol., 35, 1436 (2014).
[37] J. Mouldar, B. Hatimi, H. Hafdi, M. Joudi, M.E.A. Belghiti, H. Nasrellah, M.A. El Mhammedi, L. El Gaini, M. Bakasse, Water, Air, Soil Pollut., 231, 205 (2020).
[38] J. Mouldar, B. Hatimi, H. Hafdi, M. Joudi, M.E.A. Belghiti, H. Nasrellah, M.A. El Mhammedi, L. El Gaini, M. Bakasse, Water, Air, Soil Pollut.,231, 205 (2020).
[39] T.H. Nazifa, N. Habba, Salmiati, A. Aris, T. Hadibarata, J. Chinese Chem. Soc., 65, 259 (2018).
[40] A. El Nemr, J. Hazard. Mater., 161, 132 (2009).
[41] M. Ghaedi, A.M. Ghaedi, E. Negintaji, A. Ansari, A. Vafaei, M. Rajabi, J. Ind. Eng. Chem., 20, 1793 (2014).

HOW TO CITE THIS ARTICLE

Shabnam Alibakhshi, Ashraf S. Shahvelayati, Maryam Ranjbar, Shabnam Sheshmani, Saeid Souzangarzadeh, "**Determination of optimum amounts of effective parameters in reactive dyes removal Using a zeolitic-imidazolate framework catalyst.**" International Journal of New Chemistry., 2023; 10(1), 122-135. DOI: 10.22034/ijnc.2022.558119.1298